Vol 15 No 11, November 2006
1009-1963/2006/15(11)/2623-08

Chinese Physics

© 2006 Chin. Phys. Soc.
and IOP Publishing Ltd

Surface second harmonic generation of chiral molecules using three-coupled-oscillator model*

Wang Xiao-Ou(王晓鸥)†, Li Chun-Fei(李淳飞), and Li Jun-Qing(李俊庆)

Department of Physics, Harbin Institute of Technology, Harbin 150001*, China*

(Received 24 December 2005; revised manuscript received 7 July 2006)

Based on the three-coupled-oscillator molecular model we proposed, the relation between the second-order susceptibilities of a chiral film and the molecular hyperpolarizabilities is given. The effect of microscopic parameters on the second-order susceptibilities is simulated numerically and the difference between the efficiencies of s-polarized second-harmonic fields induced by the left- and the right-handed circularly-polarized fundamental beams is discussed. The theoretical basis for studying second-order nonlinear optical properties of the chiral molecular media with a tripod-like structure is provided in this paper.

Keywords: molecular chirality, three-coupled-oscillator model, second-order susceptibility, second-harmonic generation

PACC: 4265B, 4265K, 7820B, 7820E

1. Introduction

It is well known that second-order nonlinear optical processes are forbidden in the electric-dipole approximation, in the centrosymmetric materials,[1] whereas the chiral molecules are naturally non-centrosymmetric and hence possess the nonvanishing electric-dipole-allowed molecular hyperpolarizabilities. Moreover, the isotropic medium consisting of chiral molecules are also noncentrosymmetric with second-order susceptibilities. Therefore, second-order nonlinear optical processes (such as second harmonic generation (SHG), and so on) are sensitive probes to chiral isotropic surfaces and thin films.[2−4] Such a method has received much attention in chiral nonlinear optics.

In the study on the chiral nonlinear optics, an important work is to establish microscopic models involving classical or quantum ones. Based on the chiral molecular models, one can further investigate nonlinear optical processes of chiral molecular systems.[5−14] Furthermore, classical models can give very instructive information about the link of the molecular configuration to the nonlinear processes. Up to now, four kinds of chiral-molecular classical models have been proposed: the electron-on-helix model,[8−11] i.e. Drude's model; the two-coupled-oscillator model,[9,12] i.e. Kuhn's model; the simplified Kirkwood's model[13] and the three-coupled-oscillator model.[14]

The electron-on-helix model is used to describe the chiral molecules with a helix structure, in which the conjugated π-electrons can move along the helical path, such as helicene, stilbene, and bipyridyl etc. However, this model is too simple to describe the large molecules consisting of several separated groups. Therefore, some coupled-oscillator models with two groups have been developed, such as the two-coupled-oscillator model and the simplified Kirkwood's model. The former is concerned with the chiral molecules with two weak-coupled electric oscillation centres, which move along the directions orthogonal to each other on two parallel planes with a certain spacing, such as 1, 1′-bi-2-naphthol, tartaric acid, Tröger base etc. The last one is used to investigate the chiral molecules with two anisotropic groups, which have the same structure but different orientations.

Notice that recent years, there has been a considerable increase in synthesizing the molecules with a tripod-like structure in chemistry because of their unique chemical properties.[15−17] However, few studies on the physical characters of this kind molecules are reported. Furthermore, the above three chiral-molecule models cannot be used to analyse this kind of molecules. So we develop a new model, the three-coupled-oscillator model, to describe the chiral

*Project supported by the Natural Science Foundation of Heilongjiang Province, China (Grant No A200406).

†E-mail: wxo@hit.edu.cn

molecules with a tripod-like structure.

The second-order chiral nonlinear optics mainly focuses on second harmonic processes. Using the electron-on-helix model, Make and Persoons[8] investigated many kinds of factors that influence the efficiency in SHG both theoretically and experimentally. Hache *et al*[9] did similar studies using the coupled oscillator model. They calculated the hyperpolarizabilities of chiral molecules, and gave the relation between the hyperpolarizabilities and susceptibilities. We have also investigated the processes of SHG and sum-frequency generation (SFG) using two-coupled-oscillator model[18,19] and proposed a new model[14] to investigate the SHG on chiral molecular surface with a tripod-like structure.

In this paper, we investigate the second-order nonlinearity of the surfaces composed of chiral molecules with a tripod-like structure. We will present the circular differences in SHG signals through the second-order susceptibilities, and then introduce the relation of susceptibilities with molecular hyperpolarizabilities using the three-coupled-oscillator model. We will numerically simulate the spectra of SHG susceptibilities with various chiral molecular structure parameters. We will also discuss the relation between surface SHG efficiency and polarization states of incident fundamental light.

2. General description of surface SHG

We consider the experimental arrangement illustrated in Fig.1. A thin layer made of chiral molecules is excited by a laser beam with frequency ω at an angle $\theta_{\rm inc}$. Due to the nonlinear interactions in the thin layer, second-harmonic fields at frequency 2ω are generated in the reflected and transmitted directions. We suppose that the nonlinear response is localized within the thin layer between the surrounding bulk media, and the higher multipole contributions of the bulk media are negligible, but allow the possibility that the nonlinearity of the active material has contributions beyond electric-dipole approximation. In addition, the nonlinear layer is assumed to be sufficiently thin so that the linear effects do not mix the p- and s-polarized components of the fields.

We take the chiral surface to be in the $x-y$ plane and the fundamental field at frequency ω to be a monochromatic plane wave given by

$$\boldsymbol{E} = \boldsymbol{e}E_0(\omega)\exp[\mathrm{i}(k\cdot r-\omega t)], \tag{1}$$

where $\boldsymbol{e}$ denotes the polarization direction of light, and the amplitude $E_0(\omega)$ is assumed to be constant. This field is taken to propagate in the $x-z$ plane, wave vector of which is given by

$$\boldsymbol{k} = -\boldsymbol{e}_z k\cos\theta_{\rm inc} + \boldsymbol{e}_x k\sin\theta_{\rm inc}\,, \tag{2}$$

where $\boldsymbol{e}_x$ and $\boldsymbol{e}_z$ are the Cartesian unit vectors, $\theta_{\rm inc}$ is the angle of incidence (Fig.1(a)), and $k=\omega/c$, where c is the speed of light. Generally, an arbitrary polarization state of the incident field is conveniently expanded in the basis of the s- and p-polarized unit vectors, which are

$$\boldsymbol{e}_s = -\boldsymbol{e}_y \qquad \boldsymbol{e}_{\mathrm{F}p} = \boldsymbol{e}_x\cos\theta_{\rm inc} + \boldsymbol{e}_z\sin\theta_{\rm inc}\,, \tag{3}$$

where the subscript F refers to the fundamental field. Thus, the amplitude of fundamental field is decomposed to

$$\boldsymbol{e}E_0(\omega) = \boldsymbol{e}_s E_s(\omega) + \boldsymbol{e}_{\mathrm{F}p}E_p(\omega)\,. \tag{4}$$

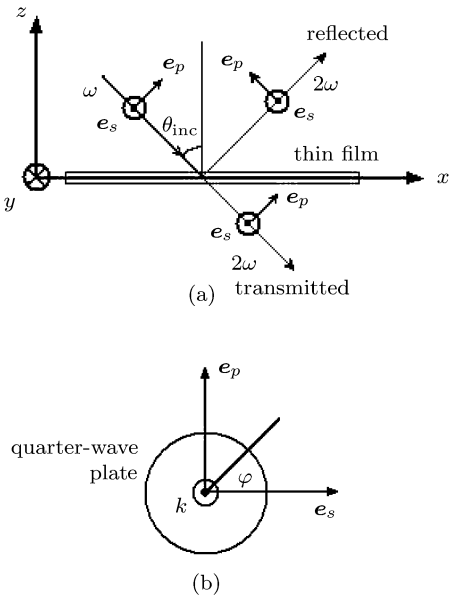


Fig.1. Second-harmonic generation from a thin film. (a) A laser beam at frequency ω is incident on the sample at angle $\theta_{\rm inc}$. Second-harmonic fields are generated in the reflected and transmitted directions. The surface normal is along the z axis. The p and s unit vectors for each fields are also shown. (b) φ is the angle between the fast axis of the wave plate and the s direction.

We next consider a situation in which a quarter-wave plate is used to control the polarization state of

the fundamental field between left- and right-handed circular. Passing through the quarter-wave plate, the amplitudes of components of the incident fundamental light are[2]

$$E_s(\omega) = E_0(\omega)\sin\varphi\cos\varphi(1-\mathrm{i}),$$
$$E_p(\omega) = E_0(\omega)(\sin^2\varphi + \mathrm{i}\cos^2\varphi), \quad (5)$$

where φ is the rotation angle of the wave plate measured as the angle between the fast axis of the wave plate and the s direction (Fig.1(b)). Note that the rotation angles of $+45°$ and $-45°$ correspond to the left- and right-handed circularly polarized incident fields, respectively.

Consider the nonlinear polarization at the second-harmonic frequency,

$$P_i^{(2)}(2\omega) = \chi_{ijk}^{\mathrm{eee}} E_j(\omega)E_k(\omega) + \chi_{ijkl}^{\mathrm{eeq}} E_j(\omega)\nabla_k E_l(\omega)\,. \quad (6)$$

The relation between the electric-field amplitudes of the fundamental and second-harmonic fields can be expressed in the general form[20]

$$E_j(2\omega) = f_j E_p^2(\omega) + g_j E_s^2(\omega) + h_j E_p(\omega)E_s(\omega)\,, \quad (7)$$

where j denotes s or p. For circularly polarized fundamental light, the ratio $E_p(\omega)/E_s(\omega)$ is $+\,\mathrm{i}$ for right-handed light and $-\mathrm{i}$ for left-handed light. The intensity of the s or p component of the second-harmonic light for circularly polarized fundamental light is[21]

$$I_j(2\omega) = |E_j(2\omega)|^2 \propto |-f_j + g_j \pm \mathrm{i}h_j|^2 I_0^2(\omega). \quad (8)$$

The difference in intensities for left- and right circularly polarized excitation light is expressed as $\Delta I(2\omega) = I_L(2\omega) - I_R(2\omega)$, where I_L and I_R refer to left and right circularly polarized excitation, respectively. We obtain

$$\Delta I_j(2\omega) \propto [\mathrm{Im}(h_j^* f_j) + \mathrm{Im}(g_j^* h_j)]I_0^2(\omega). \quad (9)$$

The nonlinear expansion coefficients f_i, g_i and h_i are different for the reflected and transmitted components of the second-harmonic field. The coefficients depend linearly on the components of the various susceptibility tensors that characterize the interaction.[22] In our model, their expressions are

$$f_{\mathrm{T}s}^{\mathrm{R}s} = 2\chi_{XYZ}^{\mathrm{eee}}\sin\theta_{\mathrm{inc}}\cos\theta_{\mathrm{inc}}\,, \quad g_{\mathrm{T}s}^{\mathrm{R}s} = 0\,,$$
$$h_{\mathrm{T}s}^{\mathrm{R}s} = 2\chi_{XXZ}^{\mathrm{eee}}\sin\theta_{\mathrm{inc}},$$
$$f_{\mathrm{T}p}^{\mathrm{R}p} = \sin\theta_{\mathrm{inc}}(\chi_{ZZZ}^{\mathrm{eee}}\sin^2\theta_{\mathrm{inc}} + \chi_{ZXX}^{\mathrm{eee}}\cos^2\theta_{\mathrm{inc}} \mp 2\chi_{XXZ}^{\mathrm{eee}}\cos^2\theta_{\mathrm{inc}}),$$
$$g_{\mathrm{T}p}^{\mathrm{R}p} = \chi_{ZXX}^{\mathrm{eee}}\sin\theta_{\mathrm{inc}}\,,$$
$$h_{\mathrm{T}p}^{\mathrm{R}p} = \mp\chi_{XYZ}^{\mathrm{eee}}\sin\theta_{\mathrm{inc}}\cos\theta_{\mathrm{inc}}, \quad (10)$$

where the superscripts (subscripts) on the left-hand side of the equations correspond to the upper (lower) signs on the right-hand side, respectively. R and T in the superscripts and subscripts refer to the reflected and transmitted directions, respectively. Thus, the difference in intensities of the second-harmonic fields $\Delta I(2\omega)$ is a function of rotation angle φ .

From the above analyses, we can see that if the polarization states and incident angle of the light are given, the intensity of SHG signals in reflected and transmitted directions only depends on the second-order susceptibilities of the media, which are related to the microscopic structure of molecules.

3. Susceptibility of surface SHG based on the three-coupled-oscillator model

The three-coupled-oscillator model is described in detail in Ref.[14]. In this section, starting from the microscopic response of individual molecules, we will obtain the hyperpolarizabilities of chiral molecules from the three-coupled-oscillator model, and give a general treatment of the SHG in an isotropic layer of chiral molecules. After averaging over all possible directions, we deduce the nonvanishing surface susceptibilities. In the process of deducing surface susceptibilities, we use the coupled equations of motion for the three oscillators, and the definition of all parameters can be found in Ref.[14].

If the molecular system is excited by a monochromatic wave with frequency ω, and the electric field can be expressed as $\boldsymbol{E}_i(\boldsymbol{r},t) = \boldsymbol{E}_i(\boldsymbol{r})\exp(-\mathrm{i}\omega t) + \mathrm{c.c.}$, the response of oscillators to the electric field includes not only fundamental frequency, but also second-harmonic and third-harmonic frequencies. We only consider the case of fundamental and second-harmonic frequencies, thus $a = a_1\mathrm{e}^{-\mathrm{i}\omega t} + a_2\mathrm{e}^{-\mathrm{i}2\omega t} + \mathrm{c.c.}$, $b = b_1\mathrm{e}^{-\mathrm{i}\omega t} + b_2\mathrm{e}^{-\mathrm{i}2\omega t} + \mathrm{c.c.}$, $c = c_1\mathrm{e}^{-\mathrm{i}\omega t} + c_2\mathrm{e}^{-\mathrm{i}2\omega t} + \mathrm{c.c.}$ (where a, b, c is the elongations of the three oscillators from their equilibrium positions).

Consider the spatial dispersion (SD) of electric field, in the vicinity of the origin O, the electric field can be readily expanded along the spatial directions

as

$$E_{ij} = E_j + \frac{\partial E_j}{\partial x}x_i + \frac{\partial E_j}{\partial y}y_i + \frac{\partial E_j}{\partial z}z_i$$
$$(i = 1, 2, 3; j = x, y, z)\,. \tag{11}$$

Adopting this first-order expansion is appropriate since the molecular extension is smaller than the wavelength of the light.

The coupled equations for second-harmonic frequency can be written as

$$D_1(2\omega)a_2 + A_{12}b_2 + A_{13}c_2 = \frac{q_1}{m_1}R_1a_1 - f_1a_1^2, \tag{12a}$$
$$D_2(2\omega)b_2 + A_{21}a_2 + A_{23}c_2 = \frac{q_2}{m_2}R_2b_1 - f_2b_1^2, \tag{12b}$$
$$D_3(2\omega)c_2 + A_{31}a_2 + A_{32}b_2 = \frac{q_3}{m_3}R_3c_1 - f_3c_1^2, \tag{12c}$$

where $D_i(2\omega) = -4\omega^2 + \omega_{0i}^2 - 4\mathrm{i}\omega\gamma_i$ and f_i are the introduced anharmonic coefficients. R_i is the linear combination of the products of electric field and its gradient, namely E_jE_k, $E_j(\partial E_l/\partial x_k)$ and $(\partial E_k/\partial x_j)E_l$.

From the coupled equations for the second harmonic motion, it is possible to calculate the induced electric dipole, which is expressed by

$$p_i^{(2)}(2\omega) = \varepsilon_0\beta_{ijk}^{\mathrm{eee}}E_j(\omega)E_k(\omega) + 2\varepsilon_0\tilde{\beta}_{ijkl}^{\mathrm{eeq}}E_j(\omega)\nabla_kE_l(\omega). \tag{13}$$

The electric dipolar moment of a molecule is

$$\boldsymbol{p} = \sum_j q_j\boldsymbol{r}_j, \tag{14}$$

where $\boldsymbol{r}_j$ are the position vectors of the oscillators, which are related to the molecular responses of the three oscillators to the electric excitation. And the expansion of electric dipolar moments for an individual molecule in the electric field is

$$p_i = p_{i0} + p_i^{(1)}\exp(-\mathrm{i}\omega t) + p_i^{(2)}\exp(-\mathrm{i}2\omega t) + \ldots + \mathrm{c.c.} \quad (i = x, y, z), \tag{15}$$

where p_{i0} is the inherent electric dipolar moment of the molecule, whereas $p_i^{(1)}(\omega)$ and $p_i^{(2)}(2\omega)$ are the first-order and the second-order induced electric dipolar moments of the molecule, respectively. From the above, we can obtain the expressions of hyperpolarizabilities β^{eee} (see appendix).

Usually, the macroscopic susceptibilities depend on the microscopic polarizabilities. For the second-order process, we have

$$\chi_{IJK}^{(2)} = Nf_{\mathrm{L}}^3\left\langle(I\cdot i)(J\cdot j)(K\cdot k)\right\rangle\beta_{ijk}^{\mathrm{eee}}\,, \tag{16}$$

where i, j, k and I, J, K refer to the molecular and the laboratory frames. $\langle\ \rangle$ represents the averaging operation. $N$is the molecular surface density; f_L^3 is the local field factor of modifications in three directions. Sometimes, the effect of local field caused by interaction of molecules is very weak. For example, the interaction of molecules in diluted media is smaller than intramolecular forces; therefore, the correction of local-field factor can be ignored.

Due to the high symmetry of the surface (C_∞) and the individual molecules, many components of the susceptibilities go to zero. We give the nonvanishing independent components for χ^{eee} in the following.

$$\chi_{ZZZ}^{\mathrm{eee}} = \frac{Nf_{\mathrm{L}}^3\cos\theta}{2}[(2\beta_{xxz}^{\mathrm{eee}} + 2\beta_{yyz}^{\mathrm{eee}} + \beta_{zxx}^{\mathrm{eee}} + \beta_{zyy}^{\mathrm{eee}})\sin^2\theta + 2\beta_{zzz}^{\mathrm{eee}}\cos^2\theta]\,, \tag{17a}$$
$$\chi_{ZXX}^{\mathrm{eee}} = \frac{Nf_{\mathrm{L}}^3\cos\theta}{4}[2(-\beta_{xxz}^{\mathrm{eee}} - \beta_{yyz}^{\mathrm{eee}} + \beta_{zzz}^{\mathrm{eee}})\sin^2\theta + (1+\cos^2\theta)(\beta_{zxx}^{\mathrm{eee}} + \beta_{zyy}^{\mathrm{eee}})]\,, \tag{17b}$$
$$\chi_{XXZ}^{\mathrm{eee}} = \frac{Nf_{\mathrm{L}}^3\cos\theta}{4}[2(\beta_{xxz}^{\mathrm{eee}} + \beta_{yyz}^{\mathrm{eee}})\cos^2\theta - (\beta_{zxx}^{\mathrm{eee}} + \beta_{zyy}^{\mathrm{eee}} - 2\beta_{zzz}^{\mathrm{eee}})\sin^2\theta]\,, \tag{17c}$$
$$\chi_{XYZ}^{\mathrm{eee}} = \frac{Nf_{\mathrm{L}}^3}{4}(2\cos^2\theta - \sin^2\theta)(\beta_{xyz}^{\mathrm{eee}} - \beta_{yxz}^{\mathrm{eee}}) \tag{17d}$$

with $\chi_{ZXX}^{\mathrm{eee}} = \chi_{ZYY}^{\mathrm{eee}}$, $\chi_{XXZ}^{\mathrm{eee}} = \chi_{XZX}^{\mathrm{eee}} = \chi_{YYZ}^{\mathrm{eee}} = \chi_{YZY}^{\mathrm{eee}}$, $\chi_{XYZ}^{\mathrm{eee}} = \chi_{XZY}^{\mathrm{eee}} = -\chi_{YXZ}^{\mathrm{eee}} = -\chi_{YZX}^{\mathrm{eee}}$, where some expressions of molecular hyperpolarizabilities β^{eee} used for surface second harmonics are shown in the Appendix. Similar expressions exist for calculating the nonlinear susceptibilities χ^{eeq}, which are quite complicated and much smaller than χ^{eee} in our model. So we will ignore χ^{eeq} in the next discussion and only

consider the electric dipolar interaction.

4. Simulation and discussion

4.1. Effect of molecular parameters on second-order susceptibilities

The nonlinear optical processes are governed by nonlinear susceptibilities of materials. Usually, one obtains an efficient frequency conversion process through modulating the optical susceptibility tensor $\chi^{(2)}$.

In the material composed of chiral molecules, there is a strong correlation between structure and nonlinear properties. In the second-order nonlinear process, the susceptibility tensor $\chi^{(2)}$ of the material is related to both the magnitude of the individual molecular nonlinearities (i.e. the first hyperpolarizability β^{eee}) and the relative distribution of molecules in the medium (see Eqs.(17a)–(17d)). The β^{eee} is connected with the parameters of molecular configuration. The aim of the study on nonlinear processes of chiral molecules is to reveal mainly the relation between microscopic parameters of chiral molecules and macroscopic characteristic of the medium for future applications (such as in sensors, nonlinear optics, and opto-electronics).

From Section 2, we know that the intensity of SHG signals in the reflected and transmitted directions can be shown to be

$$I(2\omega) = |\chi^{(2)}_{\mathrm{eff}}|^2 A\,,$$

where A is related to the intensity of incident signal, frequency, polarization states and the incident angle of the light. Moreover, we can assume that $\chi^{(2)}_{\mathrm{eff}}$ is a linear combination of the nonvanishing second-order susceptibilities $\chi^{\mathrm{eee}}_{IJK}$, which is obtained in our model. A can be regarded as a constant as long as the intensity of the incident signals, frequency, polarization states and the incident angle of the light are defined. Thus $|\chi^{(2)}_{\mathrm{eff}}|$ can be used to show the efficiency of the SHG.

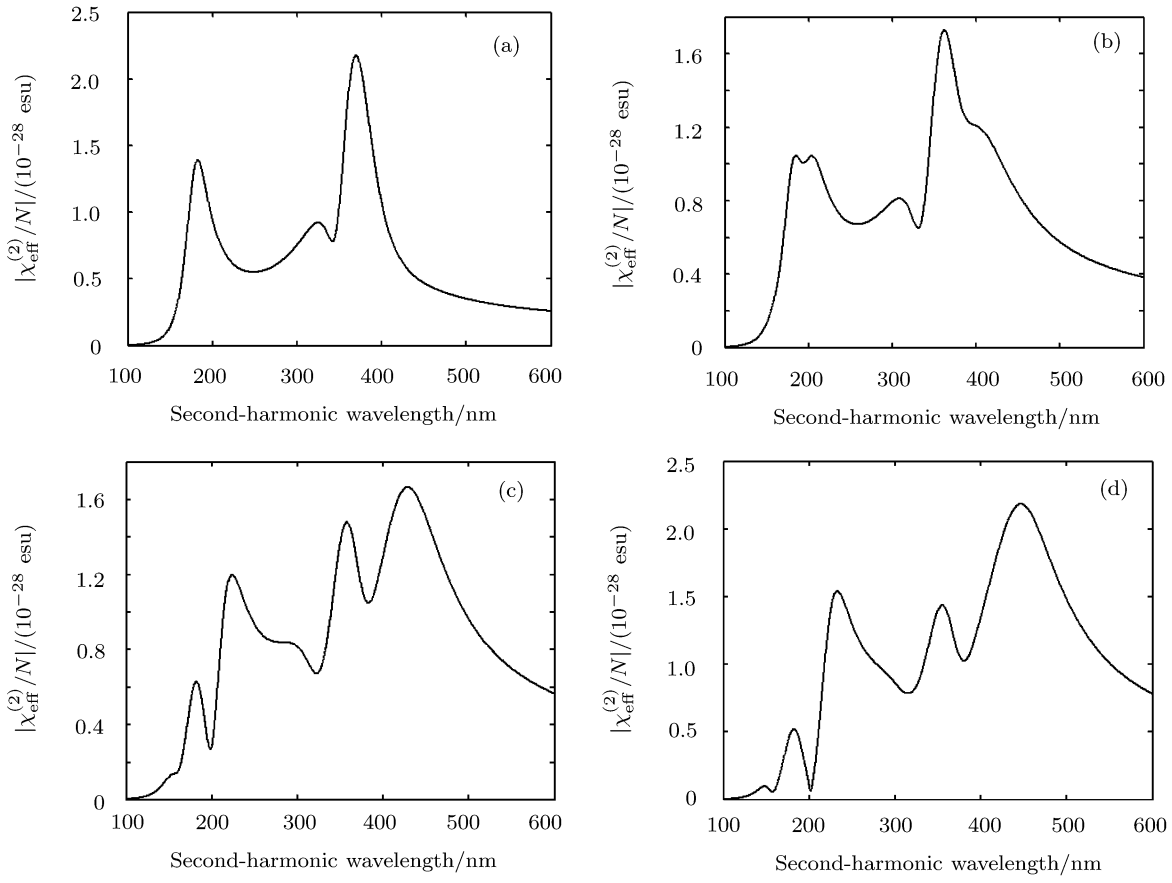


Fig.2. The plots of absolute value of $\chi^{(2)}$ versus second harmonic wavelength under the condition of different chirality. (a) Three oscillators are the same (e.g. no chirality), (b)–(d) having the following chiral components: (b) $\omega_{01}/\omega_{02} = 1.11$, $\omega_{02}/\omega_{03} = 1.11$, $\omega_{03}/\omega_{01} = 0.83$, (c) $\omega_{01}/\omega_{02} = 1.15$, $\omega_{02}/\omega_{03} = 1.18$, $\omega_{03}/\omega_{01} = 0.74$, (d) $\omega_{01}/\omega_{02} = 1.19$, $\omega_{02}/\omega_{03} = 1.24$, $\omega_{03}/\omega_{01} = 0.68$.

We assume that the wavelength of the incident fundamental light is 1064 nm. The plots of absolute value of $\chi^{(2)}_{\text{eff}}$ versus the second harmonic wavelength in the case of different chirality are given in Fig.2 (namely harmonic efficient spectra). In Fig.2(a), the three oscillators are the same (e.g. no chirality), which means that the molecular configuration is symmetric. From Fig.2(a), the three absorption peaks are related to the three inherent frequencies of oscillators; it indicates that a stronger second-order process may occur at the absorption peak of oscillators. In Figs.2(b) to 2(d), corresponding chiral relations are $\omega_{01}/\omega_{02} = 1.11,\ 1.15,\ 1.19$, $\omega_{02}/\omega_{03} = 1.11,\ 1.18,\ 1.24$, $\omega_{03}/\omega_{01} = 0.83,\ 0.74,\ 0.68$, respectively. From Figs.2(b) to 2(d), with the increase of molecular chirality, the number of peaks increases and the spectra are broadened. The phenomenon of multiple peaks shows that coupling of the three oscillators may break up the degeneracy of the three oscillators, and new optical transition frequencies are produced. The multiple peaks will help to choose a proper wavelength for the second-order susceptibility.

From the above simulation, it shows that, in the media composed of chiral molecules with a tripod-like structure, the difference of the three oscillators is augmented with the increase of chirality, which can enhance the effective second-order susceptibility, and can increase the second harmonic efficiency.

4.2. Spectra of rotation angle for second-harmonic reflection

Suppose that the incident fundamental beam is Nd:YAG laser (1064 nm) and the incident angle is 45°. The polarization states of the incident beam are continuously varied by rotating a quarter waveplate in the range from −180° to 180°. The curves for the s-polarized second-harmonic signals in the reflected and transmitted directions are shown in Fig.3.

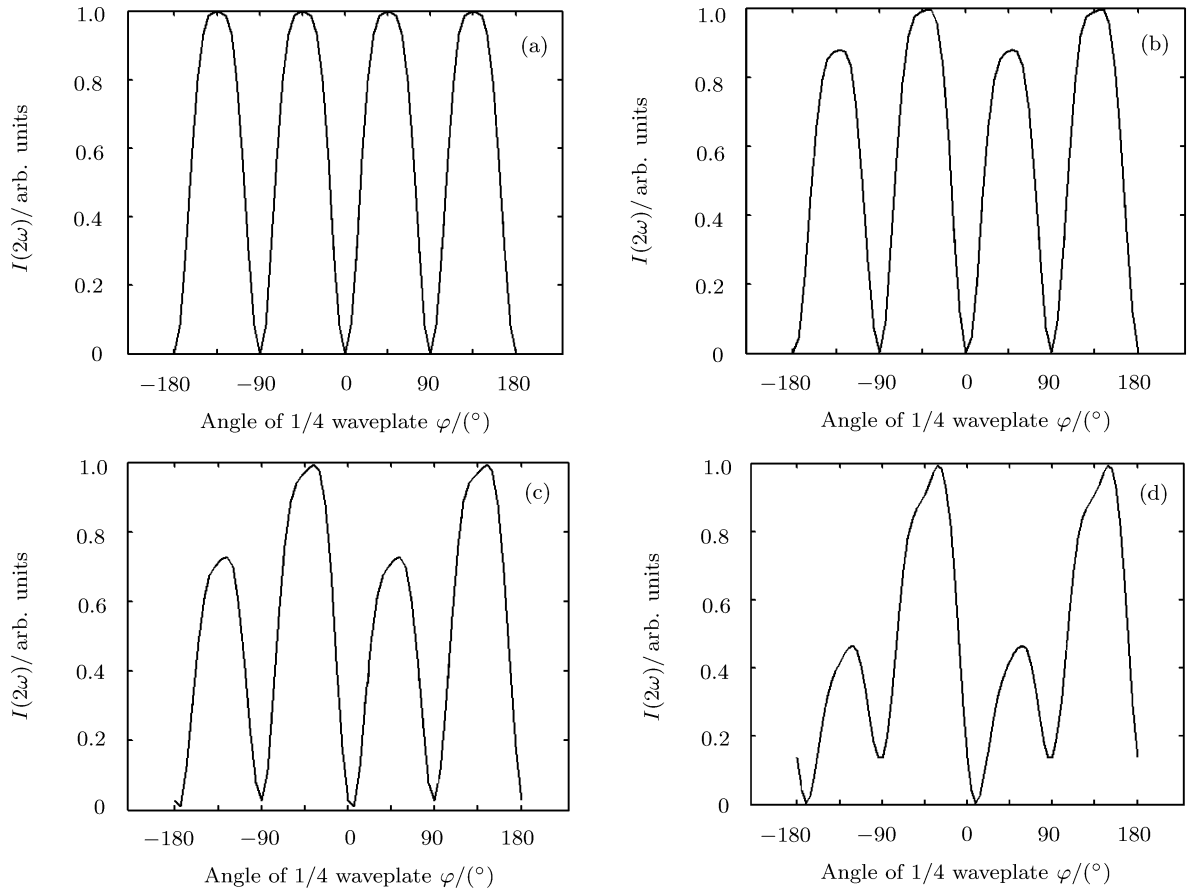


Fig.3. The intensity of the s-polarized second-harmonic field versus the angle of 1/4 waveplate φ for different chiral parameters. The rotation angles of 45°(−135°) and 135°(−45°) correspond to the two circular polarizations of the fundamental beam. (a) Three oscillators are the same (e.g. no chirality), (b)–(d) having the following chiral components: (b) $\omega_{01}/\omega_{02} = 1.04$, $\omega_{02}/\omega_{03} = 1.04$, $\omega_{03}/\omega_{01} = 0.93$, (c) $\omega_{01}/\omega_{02} = 1.11$, $\omega_{02}/\omega_{03} = 1.12$, $\omega_{03}/\omega_{01} = 0.81$, (d) $\omega_{01}/\omega_{02} = 1.13$, $\omega_{02}/\omega_{03} = 1.15$, $\omega_{03}/\omega_{01} = 0.76$.

The chirality is successively increased from Figs.3(a) to 3(d), and Fig.3(a) corresponds to the case of no chirality. The difference in efficiencies of SHG for left-hand ($\varphi = -45°$) and right-hand ($\varphi = 45°$) circularly-polarized fundamental beams becomes much evident with the augment of the chirality. This difference is a characteristic of the molecular chirality and is called circular difference or CD-SHG (respectively linear difference or LD-SHG). The obvious signature of chirality is the asymmetry of shapes of curves, which is very important for discriminating chirality.

Compared with the result obtained by using the two-coupled-oscillator model in Ref.[23], the molecular media based on the three-coupled-oscillator model have stronger coupling between molecules, and exhibit the phenomenon of multiple peaks. Its CD-SHG becomes remarkable with the increase of chirality. These indicate that the chiral molecules with a tripod-like structure have a better second-order nonlinearity.

5. Conclusion

We have studied the relation between the second-order susceptibility of chiral film and hyperpolarizabilities of molecules based on the three-coupled-oscillator model, simulated numerically and analysed the effect of microscopic parameters on the second-order susceptibilities. We also discuss the effect of chirality changes on the responses to left- and right-handed circularly-polarized (LHCP and RHCP) fundamental beams.

We can conclude that properly changing the chirality of molecules may enhance the SHG efficiency by increasing the susceptibility, which is related to the asymmetric structure of the chiral molecule. We can also predict the efficiency of and the difference between LHCP and RHCP fundamental light in second-order nonlinear processes according to the molecular structure.

Appendix

$$\beta^{eee}_{xxz} = \frac{q^3 \sin\alpha \cos^2\alpha}{4\varepsilon_0 m^2}\Big[\Big(\frac{f_1}{D_1(2\omega)D_1^2(\omega)} + \frac{f_2}{D_2(2\omega)D_2^2(\omega)}\Big)\Big(1 + \frac{A_{13}(D_3(2\omega) + 2D_3(\omega))}{D_3(2\omega)D_3(\omega)}\Big) + \frac{4f_3}{D_3(2\omega)D_3^2(\omega)} - \frac{A_{12}}{D_2(2\omega)D_1(2\omega)}\Big(\frac{f_1(D_2(\omega) + 2D_2(2\omega))}{D_2(\omega)D_1^2(\omega)} + \frac{f_2(D_1(\omega) + 2D_1(2\omega))}{D_1(\omega)D_2^2(\omega)}\Big) - \frac{2A_{13}f_3}{D_3(2\omega)D_3^2(\omega)}\Big(\frac{2D_2(2\omega) - D_2(\omega)}{D_2(2\omega)D_2(\omega)} + \frac{2D_1(2\omega) - D_1(\omega)}{D_1(2\omega)D_1(\omega)}\Big)\Big];$$

$$\beta^{eee}_{xyz} = -\frac{\sqrt{3}q^3 \sin\alpha \cos^2\alpha}{4\varepsilon_0 m^2}\Big[\Big(\frac{f_1}{D_1(2\omega)D_1^2(\omega)} - \frac{f_2}{D_2(2\omega)D_2^2(\omega)}\Big)\Big(1 - \frac{A_{13}(D_3(2\omega) - 2D_3(\omega))}{D_3(2\omega)D_3(\omega)}\Big) + \frac{A_{12}}{D_2(2\omega)D_1(2\omega)}\Big(\frac{f_2}{D_2^2(\omega)} - \frac{f_1}{D_1^2(\omega)}\Big) - \frac{2A_{13}f_3(D_1(\omega) - D_2(\omega))}{D_3(2\omega)D_3^2(\omega)D_2(\omega)D_1(\omega)}\Big];$$

$$\beta^{eee}_{yxz} = \frac{\sqrt{3}q^3 \sin\alpha \cos^2\alpha}{8\varepsilon_0 m^2}\Big[\Big(\frac{f_2}{D_2^2(\omega)D_2(2\omega)} - \frac{f_1}{D_1^2(\omega)D_1(\omega 2)}\Big)\Big(1 + \frac{A_{13}}{D_3(\omega)}\Big) - \frac{A_{12}}{D_2(2\omega)D_1(2\omega)}\Big(\frac{f_1(D_2(\omega) - 2D_2(2\omega))}{D_2(\omega)D_1^2(\omega)} + \frac{f_2(2D_1(2\omega) - D_1(\omega))}{D_2^2(\omega)D_1(\omega)}\Big) - \frac{2A_{13}f_3(D_2(2\omega) - D_1(2\omega))}{D_3^2(\omega)D_3(2\omega)D_2(2\omega)D_1(2\omega)}\Big];$$

$$\beta^{eee}_{yyz} = \frac{3q^3 \sin\alpha \cos^2\alpha}{8\varepsilon_0 m^2}\Big[\Big(\frac{f_1}{D_1(2\omega)D_1^2(\omega)} + \frac{f_2}{D_2(2\omega)D_2^2(\omega)}\Big)\Big(1 - \frac{A_{13}}{D_3(\omega)}\Big) + \frac{A_{12}}{D_2(2\omega)D_1(2\omega)}\Big(\frac{f_1}{D_1^2(\omega)} + \frac{f_2}{D_2^2(\omega)}\Big)\Big];$$

$$\beta^{eee}_{zxx} = \frac{q^3 \sin\alpha \cos^2\alpha}{4\varepsilon_0 m^2}\Big[\Big(\frac{f_1}{D_1(2\omega)D_1^2(\omega)} + \frac{f_2}{D_2(2\omega)D_2^2(\omega)}\Big)\Big(1 + \frac{A_{13}(4D_3(2\omega) - D_3(\omega))}{D_3(2\omega)D_3(\omega)}\Big)$$

$$- \frac{A_{12}}{D_2(2\omega)D_1(2\omega)}\Big(\frac{f_1(D_2(\omega)+2D_2(2\omega))}{D_2(\omega)D_1^2(\omega)} + \frac{f_2(D_1(\omega)+2D_1(2\omega))}{D_2^2(\omega)D_1(\omega)}\Big)$$
$$+ \frac{4f_3}{D_3(2\omega)D_3^2(\omega)}\Big(1 + A_{13}\Big(\frac{(D_1(2\omega)-D_1(\omega))}{D_1(2\omega)D_1(\omega)} + \frac{(D_2(2\omega)-D_2(\omega))}{D_2(2\omega)D_2(\omega)}\Big)\Big)\Big];$$

$$\beta_{zyy}^{\mathrm{eee}} = \frac{3q^3\sin\alpha\cos^2\alpha}{4\varepsilon_0 m^2}\Big[\Big(\frac{f_1}{D_1(2\omega)D_1^2(\omega)} + \frac{f_2}{D_2(2\omega)D_2^2(\omega)}\Big)\Big(1 - \frac{A_{13}}{D_3(2\omega)}\Big)$$
$$+ \frac{A_{12}}{D_2(2\omega)D_1(2\omega)}\Big(\frac{f_1(2D_2(2\omega)-D_2(\omega))}{D_2(\omega)D_1^2(\omega)} + \frac{f_2(2D_1(2\omega)-D_1(\omega))}{D_2^2(\omega)D_1(\omega)}\Big)\Big];$$

$$\beta_{zzz}^{\mathrm{eee}} = \frac{q^3\sin^3\alpha}{\varepsilon_0 m^2}\Big[\Big(\frac{f_1}{D_1(2\omega)D_1^2(\omega)} + \frac{f_2}{D_2(2\omega)D_2^2(\omega)}\Big)\Big(1 - \frac{A_{13}(D_3(\omega)+2D_3(2\omega))}{D_3(2\omega)D_3(\omega)}\Big)$$
$$+ \frac{f_3}{D_3(2\omega)D_3^2(\omega)} - \frac{D_1(\omega)+2D_1(2\omega)}{D_1(2\omega)D_1(\omega)}\Big(\frac{A_{13}f_3}{D_3(2\omega)D_3^2(\omega)} + \frac{A_{12}f_2}{D_2(2\omega)D_2^2(\omega)}\Big)$$
$$- \frac{D_2(\omega)+2D_2(2\omega)}{D_2(2\omega)D_2(\omega)}\Big(\frac{A_{12}f_1}{D_1(2\omega)D_1^2(\omega)} + \frac{A_{13}f_3}{D_3(2\omega)D_3^2(\omega)}\Big)\Big];$$

References

[1] Boyd R W 1992 *Nonlinear Optics* (San Diego: Academic) Chap.1

[2] Kauranen M, Verbiest T, Maki J J and Persoons A 1994 *J. Chem. Phys.* **101** 8193

[3] Kauranen M, Elshocht S Van, Verbiest T and Persoons A 2000 *J. Chem. Phys.* **112** 1497

[4] Sioncke S, Elshocht S Van, Verbiest T, Kauranen M, Phillips K E S, Katz T J and Persoons A 2001 *Synth. Metals* **124** 191

[5] Mesnil H, Schanne-Klein M C and Hache F 2002 *Phys. Rev.* A **66** 013802

[6] Schanne-Klein M C, Mesnil H, Hache F, Brolin T, Alexandre M, Lemercier G and Andraud C 2002 *Synth. Metals* **127** 63

[7] Han S H, Ji N, Belkin, M A and Shen Y R 2002 *Phys. Rev.* B **66** 165415

[8] Maki J J and Persoons A 1996 *J. Chem. Phys.* **104** 9340

[9] Hache F, Mesnil H and Schanne-Klein M C 2001 *J. Chem. Phys.* **115** 6707

[10] Kauzmann W 1957 *Quantum Chemistry* (New York: Academic) p616

[11] Elshocht S Van, Verbiest T, Kauranen M, Ma Liang, Chen Hua, Musick K Y, Pu Lin and Persoons A 1999 *J. Chem. Phys. Lett.* **20** 315

[12] Kuhn W and Abt Z 1929 *Phys. Chem.* B **4** 14

[13] Koroteev N I 1995 *Biospectroscopy* **1** 341

[14] Wang X O, Li J Q and Li C F 2004 *Chin. Phys. Lett.* **21** 2433
Wang X O, Li J Q and Li C F 2005 *Chem. Phys.* **320** 37

[15] Qian W and Elena Galoppini 2004 *Tetrahedron* **60** 8497

[16] Deng X B and Cai C Z 2003 *Tetrahedron Lett.* **44** 815

[17] Xia C H, Chen Z M, Wu Y Q and Song Y L 2005 *Acta Phys. Sin.* **54** 5168 (in Chinese)

[18] Xin L, Li C F, Li J Q and Zheng Y D 2000 *Chin. Phys.* **9** 910

[19] Zheng Y D, Li J Q, Xin L and Li C F 2000 *Chin. Phys. Lett.* **19** 791

[20] Kauranen M, Verbiest T, Elshocht S Van and Persoons A 1998 *Opt. Mater.* **9** 286

[21] Maki J J, Verbiest T, Kauranen M, Elshocht S V and Persoons A 1996 *J. Chem. Phys.* **105** 767

[22] Maki J J, Kauranen M and Persoons A 1995 *Phys. Rev.* **B 51** 1425

[23] Zheng Y D, Li J Q and Li C F 2003 *Acta Phys. Sin.* **52** 372 (in Chinese)